MECHANICAL DESIGN CONSIDERATIONS OF A STANDING WAVE S-BAND ACCELERATOR WITH ON-AXIS COUPLERS

S.B. Hodge, L.W. Funk and S.O. Schriber
Atomic Energy of Canada Limited
Physics Division, Chalk River Nuclear Laboratories
Chalk River, Ontario, Canada K0J 1J0

Summary

The mechanical design of S-band standing wave accelerator structures with on-axis coupling cells includes material selection, cavity design, segment production, rf tuning and brazing procedures.

Pre-assembly tuning operations have been minimized by determining segment dimensions and tolerances so that segments can easily be fabricated in a near-finished condition by a commercial machining firm. Final tuning, if necessary, is easily achieved by removal of material from the cavity wall or drift tube nose.

Considerations in choosing brazing procedures were vacuum integrity, resistivity of brazing alloy, joint thickness, alignment of the structure assembly and restriction of grain growth.

Introduction

The need for high efficiency rf accelerating structures operating at room temperature has been fulfilled for certain applications by standing-wave coupled-cavity accelerators, the side-coupled structure operating in the $\pi/2$ mode[1] being an example. Considerable development work[1-4] has been carried out on the design and fabrication of 0.8 GHz side-coupled structures resulting in the establishment of assembly criteria and procedures. Recent measurements[5] have shown that the on-axis coupled structure has a shunt impedance as high as that of the side-coupled structure. Its high efficiency and ease of assembly make it an attractive alternative.

As with other accelerating structures, the mechanical design of an on-axis coupled structure necessarily includes the production of vacuum-tight systems with cavity shapes, cooling, and dimensional tolerances determined from constraints associated with desired rf and accelerating properties. For example, the rf interface between the accelerating structure and the waveguide was designed to eliminate arcing, minimize rf losses and provide adequate coupling as well as be simple to machine and assemble.

Some of the techniques developed for side-coupled structures were applied to these 3 GHz on-axis coupled structures. Structural differences necessitated development work to establish economical and suitable fabrication procedures. The results of this work and some recommendations regarding production and brazing are given in this paper.

General Description

S-band standing wave structures were fabricated from oxygen free high conductivity (OFHC) copper segments which formed coaxial accelerating and coupling cavities as illustrated in Fig. 1. Segments with square and round outer profiles were arranged alternately to facilitate insertion of longitudinal cooling tubes into holes through the corners of each "square" segment (see Fig. 2). The tubes were brazed to the segments to provide good thermal contact. This configuration eliminated coolant-vacuum interfaces where vacuum leaks would be difficult to locate and repair, and provided uniform cooling of the structure (1.5 W/cm^2 for 0.1% duty factor and 8 MeV/m accelerating gradient). The flat sides of the "square" segments were used for aligning and mounting the assembly.

All segments had the same $\beta = 0.65$ cavity profile for reasons discussed elsewhere[5] and were produced initially with the same length of right-circular cylindrical extension to make $\beta = 1$ segments. Segments for the graded β part of the structure were simply obtained by machining the cylindrical extension to appropriate length.

Rf power is coupled into the middle accelerating cavity through a circular Al_2O_3 rf window and oval iris as shown in Fig. 3. The middle cavity was formed from two "square" segments to simplify window assembly brazing and to provide additional iris cooling.

Stainless steel flanges were brazed to each end segment for connecting external beam lines. Calculations and measurements have shown that vacuums less than 10^{-4} Pa in S-band structures up to 1.6 m in length can be maintained, without a manifold, by pumping from one end only.

To minimize beam loss, the accumulated effect of drift tube misalignment must not reduce the unobstructed cross-sectional area of the beam hole to less than 90% of the drift tube hole area. For a 1.6 m long structure this implied that the mean drift tube displacement from the structure axis could not exceed 0.4 mm. Consequently accurate stacking and brazing of the segment assembly were critical fabrication requirements.

Fabrication of Components

Segment Dimensional Tolerances

Cavity resonant frequencies are determined by geometrical dimensions, particularly the length of the drift tube nose (Fig. 2), cavity diameters and parallelism of the coupling cavity faces. A tuning tolerance of ± 500 kHz for both types of cavity and a maximum 500 kHz passband gap established the tolerances for these critical dimensions. They were ± 5 μm for the nose length and coupling cavity face parallelism across any diameter and ± 13 μm for the accelerating and coupling cavity diameters.

Uniformity of the accelerating cavity profile from segment to segment was ensured by machining the cavity outer diameter to a tolerance of ± 5 μm and machining the profile using a "Mimik Tracer" located with respect to this diameter. Rf field level errors from coupling constant differences were held to within 10% by requiring coupling differences to be less than 1%. This required machining tolerances for the slots of ± 13 μm in radius and width, and of + 0°, -0.25° in azimuth. Coupling constant uniformity was ensured by the use of a milling jig located with respect to the 10.166 ± 0.006 mm diameter drift tube hole.

Several batches of segments have been produced by a commercial machining contractor. For each batch, segment dimensions were progressively changed to achieve the desired frequencies, and tolerances were tightened to the values given above. Pre-assembly tuning has been almost eliminated resulting in a large reduction in tuning costs without increased machining costs.

Material Selection

As in other accelerator applications, the segments were made from OFHC copper because of its high electrical and thermal conductivity, low vacuum outgassing rate, machineability, reasonable cost and amenability to brazing in a hydrogen atmosphere to itself or stainless steel forming good vacuum joints.

OFHC copper is produced only in the form of continuously cast billets which are highly porous and unsuitable for accelerator applications because of poor rf properties and lack of vacuum integrity. The material must be worked by forging, rolling or extrusion to eliminate porosity and reduce grain size.

Method of Production

Three methods for producing segments were considered.

1) Forge segments from cast material to the required accelerating cavity profile and machine finish the remaining surfaces.

2) Machine segments from rolled plate or bar.

3) Forge segments from rolled plate or bar leaving a machining allowance of 3 mm over all surfaces so that oxygen inclusions and other impurities are removed during machining.

Structures were successfully fabricated from segments produced by each of the first two methods. Development work determined that correct forging temperatures (730°-830°C)[7] and proper die design were important factors in obtaining consistently fine grain structure throughout the segment.

In the second method it was found that profiles could be machined with a surface finish of 1-2 μm RMS to dimensional tolerances which would almost eliminate rf tuning. Calculations showed that a perfect surface finish would only increase the shunt impedance by 2-4%; smoother finishes would substantially increase machining costs for small shunt impedance gains.

The third method combined the best features of the first two with an extra fine grain structure. In our opinion it would be the cheapest production method if 500 or more segments are made at a time.

Brazing

Types of Joints

Most joints were copper-to-copper butt type. The remainder, with the exception of the coolant tubes, were a combination of lap and butt joints between copper and stainless steel.

The stainless steel to copper joints were brazed separately to produce the middle or iris cavity assembly and the two end segment assemblies.

Copper-to-Copper Joints

Step brazing, a technique which uses a number of alloys with different melt temperatures, was used to fabricate the first group of S-band accelerating structures[5,6]. Some of the components were exposed to seven braze heats, necessitating a wide range of alloy melt temperatures. The simpler coaxial design of the on-axis coupled structures, and the absence of a vacuum manifold, reduced the number of heats required.

Experiments were made with two alloys commonly used in joining OFHC copper; gold-copper (50Au-50Cu) and silver-copper (72Ag-28Cu), to determine the ability of a single alloy to withstand repeated reheats and the metallurgical effects on the copper. All joint surfaces were machined to 1 μm RMS finish. Each joint was hydrogen brazed using 50 μm thick annular foils with a different pressure applied to the joint, ranging from 15 kPa to 60 kPa. For each alloy, eight segments were brazed, one joint at a time. Thus, the first two segments were exposed to seven heats and the eighth segment to one heat.

An etched cross section[8] of the joints brazed at 1010°C with 50Au-50Cu is shown in Fig. 4. The joints were 50 (+0, -8) μm thick, equal within tolerance to the original alloy thickness. The different pressures used had no effect on joint thickness. Only one joint had a vacuum leak which was repaired during a subsequent braze with a patch of alloy.

After three heats of 1010°C the grain structure grew so much that in some areas two large grains, if located adjacently, could span the thickness of the wall between vacuum and atmosphere. Gas diffusion along grain boundaries and the possibility of cracking because of mechanical or thermal stress would then threaten vacuum integrity.

A similar etched cross section of the joints brazed at 795°C with 72Ag-28Cu alloy is shown in Fig. 5. Grain size after seven heats is still relatively small compared to that shown in Fig. 4. All joints were leak tight. Five gaps had zero width, one was 2 μm wide and one was 7 μm wide.

Sections of each type of alloy joint were polished and studied under a microscope. 72Ag-28Cu alloy thoroughly wetted the entire joint area and diffused into the parent metal, indicative of a high strength joint. 50Au-50Cu alloy did not diffuse into the parent metal, nor did it fully wet the joint area.

These tests show that 72Ag-28Cu is the preferred alloy. 50Au-50Cu is considered unsatisfactory because of excessive grain growth, joint thickness and lower joint strength. The silver-copper alloy is also considerably cheaper. Alignment of the accelerating structure is dependent on variations in joint thickness; metal-to-metal contact is desirable.

Dimensions of 72Ag-28Cu alloy foil for segment-to-segment joints were determined by further brazing tests using as the criterion minimum alloy flow into the cavity. Preformed washers (50 μm thick) of a single size, suitable for both accelerating and coupling cavity joints, were the most effective and economic solution.

Lap joints were used for brazing coolant tubes into the "square" segments providing efficient heat transfer. The alloy requirements were good thermal conductivity, a viscosity such that the gap around the tube was filled, and a braze temperature less than 795°C. Wire rings of 80Cu-15Ag-5Pd alloy were used at a braze temperature of 735°C.

Copper-to-Stainless Steel Joints

Since 72Ag-28Cu alloy was preferred for copper-to-copper joints, an alloy for brazing copper to stainless steel at a temperature of 795°C or only slightly higher was desired to avoid excessive copper grain growth. About 5% of copper-stainless steel joints leaked in a set of tests using 72Ag-28Cu alloy. Another series of tests using 68Ag-27Cu-5Pd alloy at a brazing temperature of 835°C had a similar percentage of leaking joints. At approximately 800°C a hydrogen dew point of -60°C is necessary to reduce the oxide layer on stainless steel. It was concluded that the hydrogen in the brazing furnace retort was only marginally reducing.

Vacuum leaks were eliminated by nickel plating stainless steel brazing surfaces and brazing to copper using 68Ag-27Cu-5Pd at 835°C. The quality of the nickel plating is acceptable if blistering is not evident after firing at 635°C.

Electrical Conductivity of Brazing Alloys

For segment-to-segment brazing the electrical conductivity of the brazing alloy is important because alloy may deposit on the rf conducting surfaces. Figure 6 shows the electrical resistivity of the brazing alloys as a function of the percentage of copper in silver and gold[9].

50Au-50Cu alloy is subject to resistivity changes resulting from changes in composition by diffusion or separation by liquation through a brazing cycle. The electrical resistivity of the remaining alloy can be unacceptably high (up to 8 times that of OFHC copper), therefore alloy should not be allowed to flow over conducting surfaces. The large dark band of gold alloy (2 mm wide) shown on the rf conducting surface at the joints in Fig. 4 could reduce the shunt impedance by up to 15% depending on its composition.

72Ag-28Cu alloy is not subject to separation by liquation, but alloy composition may change because of different diffusion rates. Since its resistivity is at most 15% higher than that of OFHC copper, some alloy flow on the rf conducting surfaces can be tolerated.

Structure Alignment

Factors affecting alignment are:

1. dowel hole clearance (± 50 μm)
2. segment face parallelism (± 2 μm)
3. brazed joint parallelism[a] (50 μm - 50Au-50Cu, 0 μm - 72Ag-28Cu)
4. concentricity of drift tube holes and dowel pins (± 37.5 μm).

A Monte-Carlo computer program using the above factors calculated misalignment and unobstructed fraction of the drift tube hole areas of more than 1000 randomly stacked assemblies consisting of 31 accelerating cavities. Variable dimensions were distributed randomly within the limits given. The maximum, mean and median displacement and the minimum, mean and median percentage unobstructed fraction of the drift tube hole areas are given in Table 1, for both alloys. 72Ag-28Cu alloy is superior because displacements are smaller and unobstructed fractions are higher.

Table 1

Displacements and Percentage Unobstructed Fractions of Drift Tube Holes in Assemblies with 31 Accelerating Cavities

	Results using 50Au-50Cu	72Ag-28Cu
Maximum Displacement	1.69 mm	0.74 mm
Mean Displacement	0.81 mm	0.37 mm
Median Displacement	0.86 mm	0.38 mm
Minimum Fraction of Hole	78%	90.5%
Mean Fraction of Hole	90%	95%
Median Fraction of Hole	89%	95%

Brazing Procedure

Cleaning procedures for individual components prior to brazing included freon vapour degreasing, two acetone rinses and a final alcohol rinse. Brazing alloy was rinsed in acetone and stored in alcohol until used.

[a] Not discussed in this paper is the fact that we have noticed wedging of the brazed joints if metal to metal contact is not obtained.

Two "square" segments were brazed to form the iris cavity. The iris cavity was then machined to fit the rf window adaptor and another braze followed to complete the sub-assembly, shown in Fig. 3. Brazing with 68Ag-27Cu-5Pd made it possible to cantilever the rf window adaptor during the main segment assembly braze without the risk of remelting the sub-assembly alloy in the event of a main assembly braze temperature overshoot and without the need for jigging to support the sub-assembly.

A conventional fixed base hydrogen furnace was used for the main assembly braze (Fig. 7). A stainless steel stool with machined upper surface was levelled on the furnace base to support the segment assembly. Two layers of asbestos cloth were placed on the stool to form a thermal barrier and to prevent flow of alloy between the bottom segment and stool. A precision straight edge was used during stacking to check column alignment.

Since the 1.6 m stacked assembly formed a slender and relatively unsteady column, a pendulum type jig (Fig. 7) was used during the braze cycle. This form of jigging was not affected by thermal stressing, allowed the assembly to expand and contract with complete freedom, and maintained a constant load throughout the entire brazing cycle. The assembly temperature was brought to within 25°C of the braze temperature and held until equilibrium was reached. The assembly temperature was then quickly raised to 795°C; when the assembly reached this temperature the furnace heating bell was removed immediately. The final assembly step was installation and brazing of coolant tubes in a second heat at 735°C. Structures brazed by this method have shown no detectable vacuum leaks.

Excessive running of 72Ag-28Cu alloy occurs if the alloy is in a molten state for more than 20 minutes and also if the temperature exceeds 805°C. Typical brazing temperatures ranged from 795°C to 802°C with an average 4°C temperature difference over the assembly length as recorded by six equally spaced thermocouples. The alloy was normally in a molten state for only 15 minutes.

Conclusions

Development work on on-axis coupled S-band standing wave structures has led to reliable and economical production techniques which may be useful for other types of structure. Fabrication tolerances, based on desired characteristics of the accelerating structure, have been met with a resulting reduction in tuning. Alternating segments of "round" and "square" profile has provided a convenient means for cooling and supporting the structure.

Tests have shown that 50Au-50Cu alloy is inferior to 72Ag-28Cu alloy for this application because of joint thickness after brazing, its poor electrical conductivity and excessive grain growth resulting from the high brazing temperature. Brazing with 72Ag-28Cu alloy resulted in much less copper grain growth and produced joints that were mechanically and electrically sound, vacuum tight and did not perturb alignment.

References

1. E.A. Knapp, B.C. Knapp and J.M. Potter, Rev. Sci. Instr., 39, 979 (1968).
2. H.G. Worstell, Proc. of 1966 Linac Conf., LA-3609, 169 (1966).
3. H.G. Worstell, Proc. of 1968 Proton Linac Conf., BNL-50120, 1 (1968).
4. J. McKeown, H.R. Schneider and S.O. Schriber, Proc. of 1972 Proton Linac Conf., LA-5115, 233 (1972).
5. S.O. Schriber, L.W. Funk and R.M. Hutcheon, Proc. of this conference.
6. S.O. Schriber, E.A. Heighway and L.W. Funk, Proc. of 1972 Proton Linac Conf., LA-5115, 140 (1972).
7. J.R. Ambler, CRNL, private communication.
8. C.J. Scully, CRNL, private communication.
9. E.W. Washburn, International Critical Table of Numerical Data, Vol. VI, McGraw-Hill Book Company Inc., New York and London, 160 (1929).

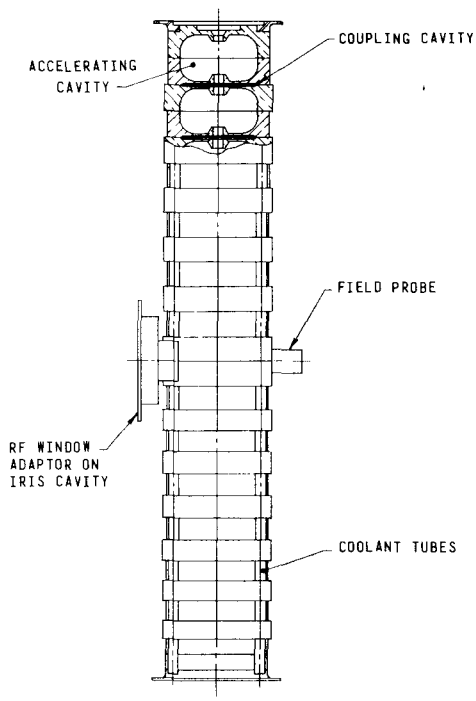

Fig. 1. S-band on-axis coupled accelerating structure showing the location of the rf window and a cross section of an accelerating and coupling cavity.

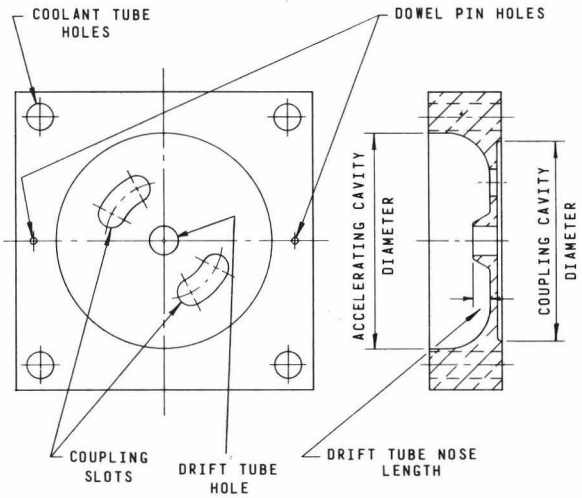

Fig. 2. Detailed views of a "square" segment.

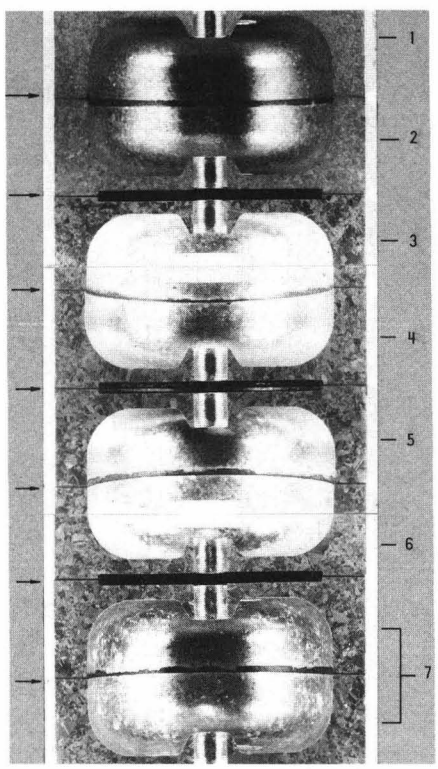

Fig. 4. Longitudinal section of 8 segment assembly brazed joint-by-joint at 1010°C in successive heating cycles - the number indicates the number of cycles each segment experienced. The arrows indicate the joint location.

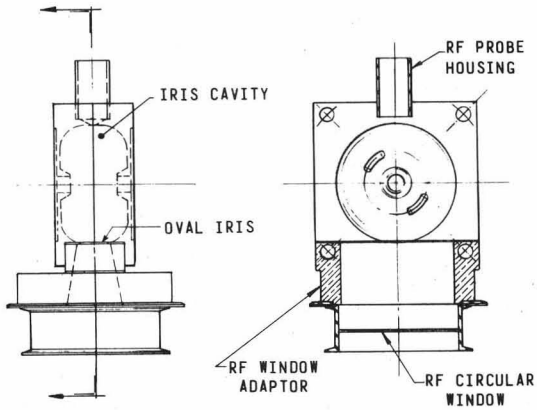

Fig. 3. Detailed views of the iris cavity, window adaptor and rf window.

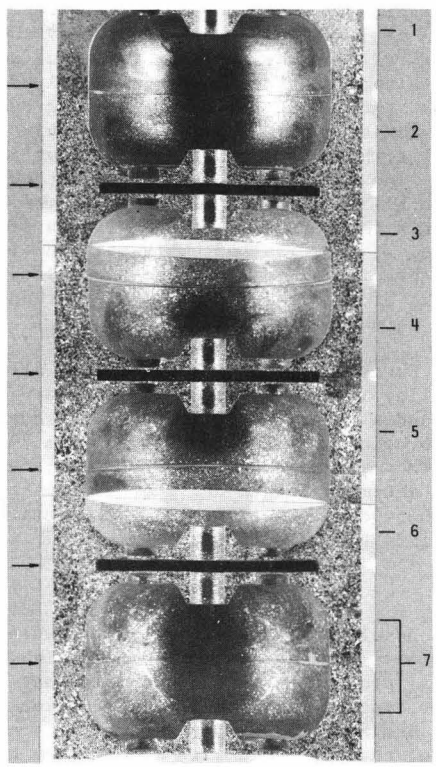

Fig. 5. Longitudinal section of 8 segment assembly brazed joint-by-joint at 795°C in successive heating cycles - the number indicates the number of cycles each segment experienced. The arrows indicate the joint location.

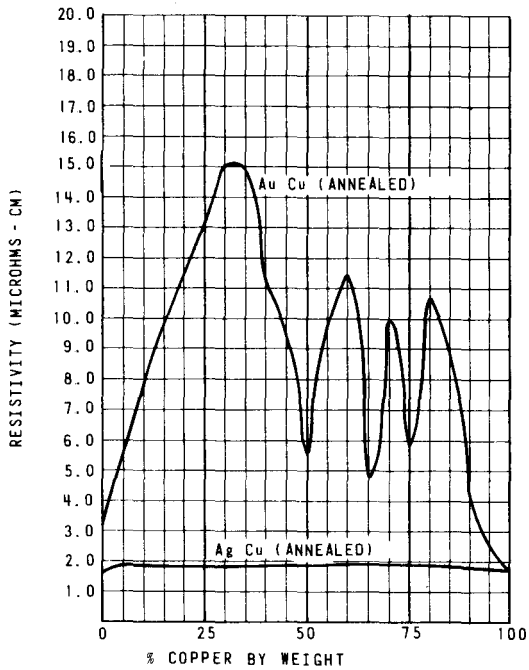

Fig. 6. Resistivity of brazing alloy as a function of copper content.

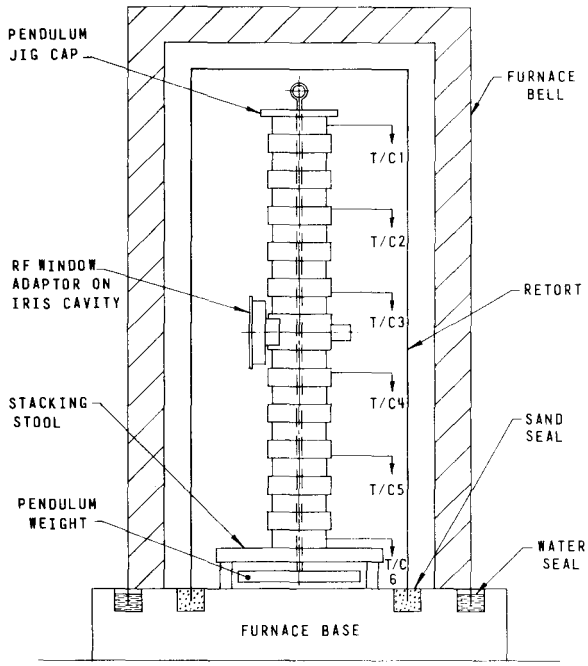

Fig. 7. Hydrogen furnace brazing arrangement.